Mon. Not. R. Astron. Soc. **000**, 1–14 () Printed 25th June 2014 (MN LATEX style file v2.2)

Multiwavelength search for counterparts of supersoft X-ray sources in M31

E. Chiosi,[1] M. Orio,[1,2], F. Bernardini[3,4], M. Henze[5], and N. Jamialahmadi[6]
[1] *INAF–Osservatorio di Padova, vicolo dell' Osservatorio 5, I-35122 Padova, Italy*
[2] *Department of Astronomy, University of Wisconsin, 475 N. Charter Str., Madison WI 53704*
[3] *Department of Physics & Astronomy, Wayne State University, 666 W. Hancock St., Detroit, MI 48201, USA*
[4] *INAF, Osservatorio di Capodimonte, Salita Moiarello, 16, 81131 Napoli, Italy*
[5] *European Space Astronomy Centre, P.O. Box 78, E-28691 Villanueva de la Canada, Madrid, Spain*
[6] *Observatoire de la Cote Azur, Boulevard de l'Observatoire, 06300 Nice, France*

arXiv:1406.2229v2 [astro-ph.SR] 24 Jun 2014

Accepted . Received; In original form

ABSTRACT

We searched optical/UV/IR counterparts of seven supersoft X-ray sources (SSS) in M31 in the Hubble Space Telescope (HST) "Panchromatic Hubble Andromeda Treasury" (PHAT) archival images and photometric catalog. Three of the SSS were transient, the other four are persistent sources. The PHAT offers the opportunity to identify SSS hosting very massive white dwarfs (WD) that may explode as type Ia supernovae in single degenerate binaries, with magnitudes and color indexes typical of symbiotics, high mass close binaries, or systems with optically luminous accretion disks. We find evidence that the transient SSS were classical or recurrent novae; two likely counterparts we identified are probably symbiotic binaries undergoing mass transfer at a very high rate. There is a candidate accreting WD binary in the error circle of one of the persistent sources, r3-8. In the spatial error circle of the best studied SSS in M31, r2-12, no red giants or AGB stars are sufficiently luminous in the optical and UV bands to be symbiotic systems hosting an accreting and hydrogen burning WD. This SSS has a known modulation of the X-ray flux with a 217.7 s period, and we measured an upper limit on its derivative, $| \dot{P} | \lesssim 0.82 \times 10^{-11}$. This limit can be reconciled with the rotation period of a WD accreting at high rate in a binary with a few-hours orbital period. However, there is no luminous counterpart with color indexes typical of an accretion disk irradiated by a hot central source. Adopting a semi-empirical relationship, the upper limit for the disk optical luminosity implies an upper limit of only 169 minutes for the orbital period of the WD binary.

Key words: binaries: close, galaxies: individual: M31, galaxies: stellar content, ultraviolet: stars, white dwarfs, X-rays: stars

1 INTRODUCTION

Supersoft X-ray sources (SSS) emit X-rays primarily at energy below 0.8 keV and with bolometric luminosity from about 10^{36} erg s^{-1} to a few times 10^{38} erg s^{-1}, and many of them have unabsorbed luminosity $> 10^{37}$ erg s^{-1}. In first approximation, the spectrum can be fitted with a blackbody at temperature from 10^5 to 10^6 K.

The first SSS were discovered with Einstein (Long, Helfand & Grabelsky 1981), and established as a class thanks to ROSAT (see Greiner 2000a). They are defined phenomenologically, and although some supernova remnants (SNR), black holes in binaries and even background active galactic nuclei (AGN) may appear as SSS, the vast majority of the SSS identified at other wavelengths turned out to be white dwarfs (hereafter WD; see e.g. Orio et al. 2010, Orio 2013). Very young single WD, PG1059 stars or planetary nebulae nuclei, may be SSS for a few years. However, because the atmosphere of an accreting and hydrogen burning WD becomes extremely hot, and can peak in the X-rays, most SSS are WD in close binaries (hereafter CBSS). In fact, more than half of the CBSS are post-outburst novae with short lived SSS phase (1 week to 10 years; see discussion of Pietsch et al. 2006; Orio 2012). CBSS comprise also some steady sources, that have remained X-ray luminous for most of the time in the last ≃30 years. The first observations of optically identified CBSS indicated that the X-ray emission was indeed due to the central source. The X-ray gratings have revealed WD atmospheres at extremely high temperature, close to a million K for post-outburst novae (see review by Orio, 2012), but also sources at lower effective temperature $T_{\rm eff}$, bordering with the EUV range. Moreover, in some novae in outburst and in a few persistent CBSS, the stellar continuum is not observed. In fact, a complex

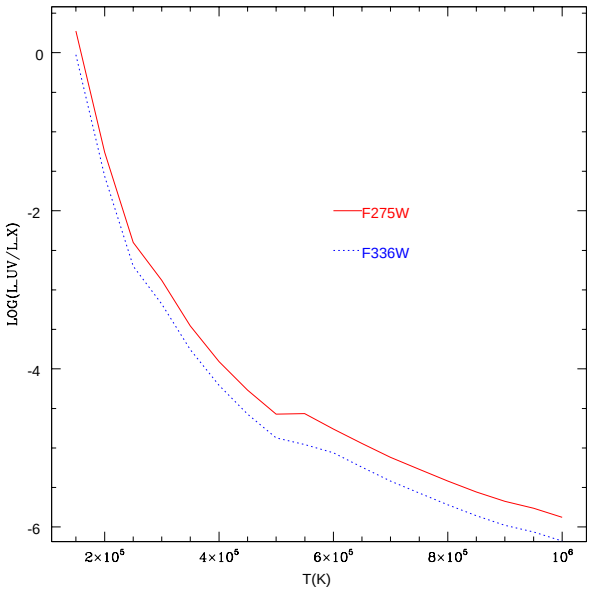

Figure 1. Ratio of WD flux in the F275W filter UV range and flux in the 0.2-1 keV X-ray range (red) and ratio of WD "U" flux in the F 336W filter and flux in the 0.2-1 keV X-ray range (blue) for a given effective temperature of the WD atmosphere, here approximated with a blackbody.

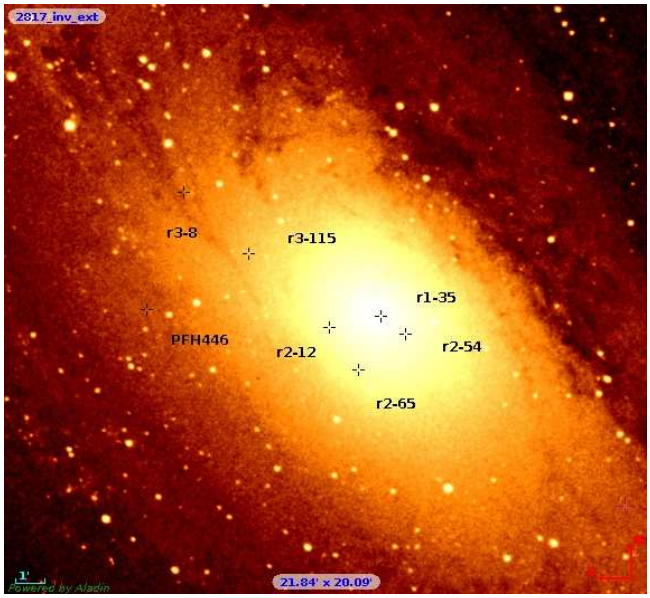

Figure 2. Positions of the SSS examined in this article in M31 on an Asiago photographic plate taken by the late L. Rosino (East is on the left and North on top). The center of the Figure is at equatorial coordinates α_{2000}=00,43,06.58 and δ_{2000}=41,13,46.98.

emission spectrum with prominent emission lines in the supersoft X-ray range may mimic a stellar continuum, (e.g: MR Vel, Bearda et al. 2002, Motch et al. 2002, or CAL 87, see Greiner et al. 2004, Orio et al. 2004), but in broad band spectra of CCD-type detectors the emission lines are not resolved (see Orio 2012). This type of X-ray spectrum has been attributed to mass outflows or to the nova wind shocking circumstellar material (see e.g. Ness et al. 2005; **?**). The central source temperature in some of these cases has been estimated to be in the range T_{eff}=30,000-150,000 K, but it may be difficult to determine, depending much on intrinsic absorption.

We know that most SSS are post-outburst novae, or other interacting white dwarf (WD) binaries; much less often SSS have turned out to be SNR or AGN (see Orio et al. 2010). In order to cast light on the nature of the sources we need to identify their counterparts at other wavelengths. The majority of the Galactic or Magellanic Clouds SSS, including those that have not been observed in a nova eruption and seem to be permanent sources, are binary systems with a WD accreting hydrogen rich material from a companion and burning hydrogen in a thin shell. These system may be type Ia Supernovae (SNe Ia) progenitors and have attracted attention for this reason. Novae and SNe Ia undergo similar evolution. In both cases the WD accretes material on the surface, but in the first case the hydrogen accumulated on the surface reaches fusion into helium resulting in envelope ejection and rise in optical magnitude by at least 8 mag, without disintegration of the WD, while in the second case the Chandrasekhar mass limit is reached, causing a global explosion. It is unlikely that the majority of novae end as SNe Ia, although a few recurrent novae (RN; novae with repeated outbursts during a century) are promising SNe Ia progenitors' candidates due to their high WD mass.

M31 is the most massive galaxy in the Local Group and has a distance modulus Δm-M=24.45 (Dalcanton et al. 2012). It has been extensively observed in X-rays with ROSAT, Chandra and XMM-Newton, and it hosts a conspicuous population of SSS. The number of observed SSS was already of the order of a hundred in 2009 (see Orio et al. 2010, and references therein), while for comparison in the much closer Magellanic Clouds, only 29 SSS have ever been detected. A little more than a half of the SSS in Andromeda have turned out to be post-outburst novae, and two of them are SNR (Orio et al. 2010, and references therein). The nature of many others is still unknown. In this paper we search optical/UV/IR counterparts for seven sources whose fields have already been observed in the PHAT (Dalcanton et al. 2012). Only one of them has a possible nova counterpart, while others have never been identified with novae. The coordinates of the sources, the HST exposures and epochs of X-ray detections or non-detections are given in Table 1.

The rest of the paper is organized as follows: in Section 2 we discuss the PHAT, the positional and photometric errors of its catalog, and the potential to observe SSS in its deep images. We also explain which specific types of CBSS we can expect to observe. In Section 3 we present the characteristics of the SSS with optical counterparts in the PHAT and analyse the short term variability of the most luminous and better observed of these sources, r2-12. In Section 4 we present the photometric results, obtained by matching the public PHAT catalog in the different filters. The catalogs differ slightly in positions and the fields are very crowded, so we had to accurately match the sources observed in the different filters. In Section 5 we discuss the possible counterparts or lack of thereof, and Section 6 contains our conclusions.

2 THE PHAT, A PRECIOUS RESOURCE

The HST archival data we used are the PHAT images and catalog (Dalcanton et al. 2012). The PHAT is an HST multi-cycle Survey of Andromeda, at present in its third year, that at completion will have imaged 1/3rd of the M31 star forming disk, covering a contiguous one square degree area in 828 orbits, with 6 different filters: 2 optical ones (F475W and F814W) used with the ACS/WFC camera, 2 ultraviolet ones (F275W and F336W) used with the WFC3/UVIS

camera, and 2 infrared filters (F110W and F160W) used with the WFC3/IR camera.

The survey area is divided in several so called "Bricks" which in turn contain different "Fields". As Table 1 shows, most SSS counterparts we searched are located in Brick 1 that covers the central (and obviously very crowded) region of M31. Source r3-8 is located instead in Brick 7. We used the VEGA magnitudes of the photometric catalog published by the PHAT collaboration (http://archive.stsci.edu/pub/hlsp/phat/). The likely optical counterpart of one of the SSS is also detected in the Local Group Survey (LGS, see Massey et al. 2006).

The astrometric accuracy gives an absolute error of 100 mas (dominated by errors in the ground based reference catalog) and an error of 10 mas in the relative positions of objects detected in all the three cameras.

The photometric measurements are obtained with a 50% completeness at signal to noise of 4 at F275W=25.1, F336W=24.9, F475W=27.9, F814W=27.1, F110W=25.5, F160W=24.6 for single pointings in the uncrowded outer disk. In the inner disk the optical and the NIR data are crowding limited and the deepest reliable magnitudes are up to 5 mag brighter (Dalcanton et al. 2012). In this paper we will not make use of the F160W filter, for which the photometric catalog errors are large and crowding is severe in the central region of M31 in which our SSS are located. The photometric median errors for given measured magnitudes are given by Dalcanton et al. (2012) in their Fig. 13, upper left panel, for Brick 1 in which 6 of the sources are located. Source r3-8 is instead in Brick 7, which has similar errors to Brick 9 (upper right panel of Fig. 13 in the Dalcanton et al. paper). Basically, while the measurements are crowding-limited in the optical and IR filters, in the U and UV UVIS filter the measurements are limited by photon counting. Therefore, the UVIS photometric accuracy is not strongly dependent on crowding. The median error is always larger than 0.01 mag in the F275W filter, but it is still smaller than 0.02 mag up to Vega magnitude ≈23.8 in the F475W filter. However, the median errors are large above approximately 24th magnitude; specifically, above Vega magnitude 25, the median error is larger than 0.2 mag in the F275W filter, it is close to 0.2 mag in the F336W and F814W filters, and it is about 0.1 mag in the F475W filter, for which the best precision is obtained.

2.1 CBSS detectable in the PHAT

In M31 we have to rely mainly on photometry to identify possible counterparts of X-ray sources, because most optical counterparts are too faint for ground based optical spectroscopy with the current facilities.

The PHAT is of high interest for the study of SSS in M31, because the upper limits for detection above the 4σ level, reported above, are sufficiently deep to reveal interacting binaries accreting through a disk (or even via a wind in the case of symbiotics), with $\dot{m} \geqslant 10^{-8}$ $M_\odot$ year^{-1} necessary for steady nuclear burning. The effective temperature of an accreting and hydrogen burning WD varies in a large range depending on WD mass, mass transfer rate $\dot{m}$, and on whether the source is observed after a thermonuclear flash (Starrfield et al. 2012). The WD itself would be detectable above the PHAT upper limits for the F275W and F366W filters without further contribution of an accretion disk or a symbiotic nebula only if it is on the low side of effective temperature distribution, with $T_{\rm eff} \leqslant$200,000 K. This can clearly be seen in from Fig. 1, where assuming the blackbody approximation for the atmosphere, we show how the ratio of X-ray flux to U/UV flux dramatically changes with the blackbody temperature. Above about 200,000 K the WD is so hot, that the Raleigh Jeans tail of the flux distribution moves to the far and then to the extreme UV.

In fact, all the Magellanic Clouds SSS known to be CBSS with a hydrogen burning WD have visual magnitude $M_V \leqslant 1.3$, which translates into V=25.75 in M31, or slightly fainter due to reddening (see measurements listed by Orio et al. 1994a; Šimon 2003). The brightest non-symbiotic known CBSS in both X-rays and optical is CAL 83, although at optical wavelengths RX J0513.9-6809 is of comparable magnitude and sometimes more luminous. For CAL 83 MACHO and OGLE light curves have been published (Greiner & Di Stefano 2002; Rajoelimanana et al. 2013). Assuming a distance modulus to the LMC $\Delta(m)$=18.47 (Freedman et al. 2012) and A_V=0.249 (Burstein & Heiles 1982), we find that the V magnitude varies between V=-0.92 and V=-2.02, due to a a 0.4 mag orbital magnitude amplitude superimposed on additional, discrete steps in average magnitude in three different "states" (high, intermediate and low). Simultaneous multi-color light curves in all the states have not been measured, but low states Šimon (2003) reports $(U-B)_0 \simeq$-1.17 and $(B-V)_0 \simeq -0.05$. We do know that at least the V and R magnitudes decrease or increase by the same amount in the different states (Greiner & Di Stefano 2002). Clearly, a source like CAL 83 would easily be picked up in the PHAT.

Šimon (2003) tried to to characterize the color indexes of all the SSS known in the Galaxy and the Local Group as a class. Not all the objects included by Šimon are of interest as examples for our search, because the author included in his Table 1 objects he calls "VSS", which have never been observed in X-rays as SSS and may be luminous only in the far UV. V751 Cyg, a VY Scl star, is defined as a SSS only because it showed a "softish" spectrum in an observation done with the HRI (Greiner 2000b), but the spectral resolution was very poor and the source was underluminous for an SSS. We know now that variables of this class generally are not SSS in the low state (Zemko & Orio 2013). The symbiotics listed by Šimon were not observed in X-rays, although they were selected because they show indications of a very hot central source. The general indication we draw from this paper are that the majority of known SSS in the Galaxy and in the Magellanic Clouds would be observable in the PHAT if they were at M31 distance, although some measurements may have large errors (see Fig. 3).

A very interesting results of the study of SSS in the Local Group in recent years has been the discovery of SSS in high mass X-ray binaries containing a WD (see review by Orio 2013, and references therein). Novae eruptions are observed in binaries with low mass companions, but no known evolutionary effect works against the formation of stable accretion in high mass binaries with a WD, which would have outbursts of smaller amplitude. We know now that hydrogen burning in high mass WD binaries must be instead relatively common, since four SSS in the Magellanic Clouds have been identified with massive binaries. Of these systems, only MAXI J0158-744 in the SMC was observed to undergo an optical brightening at the time of the X-ray flare (Li et al. 2012). For a significant number of SSS in M31 the only possible counterparts detected so far are hot O and B stars (see Orio et al. 2010), suggesting that there a large class of SSS host a WD and a young, hot massive companion (thus, they are High Mass X-ray Binaries, or HMXB).

The other subclass of SSS that should really easily stand out in the PHAT are the symbiotics, with their large luminosity. In the optical and IR we detect all AGB and red giant stars in the PHAT. In order to select criteria to identify possible symbiotic counterparts, we report the available photometric measurements for symbiotics that have been observed as SSS in the first four columns of Table

2. We later compare them with possible counterparts that are U/UV luminous, also included in the Table. Most interesting are those symbiotics which we believe host a steady burning WD: they are not only blue objects, but they are also "red", hosting a red giant, supergiant or AGB secondary. The colors and the optical and UV luminosity of the three known SSS-symbiotics stand out, because they are very different than those of most other stars. The large luminosity in the B and U filter is due to a bright accretion disk or at times only to a wind from which the WD accretes, because the donor star must supply the hydrogen rich material to the WD at a rate at or above 10^{-8} $M_{\odot}$ year^{-1}. These symbiotics appear at least as hot and blue as A type stars, but usually have lower luminosity than A-type stars in the V filter.

Concerning the transient SSS, a classical nova that has returned to quiescence would remain undetectable in the PHAT, but a recurrent nova (RN) in a symbiotic system would still be observable at quiescence. The difficult problem is how to identify it only on the basis of color indexes. In the Galaxy more than half of the observed RN are in symbiotics of the RS Oph type. What do these objects look like after hydrogen burning has ceased? If they accrete through a disk, the accretion disk is no longer irradiated, and the surrounding nebula is not photoionized anymore by an extremely hot central source. "Normal" symbiotics that are not known to be undergoing hydrogen burning, or where the WD is obscured by heavy intrinsic absorption, are still luminous objects in many wavelengths. Their colors are different from the ones of the luminous cool component alone, but there is a large spread in the range of magnitudes and color indexes. They are luminous in the red filters, but also in the F475W and U/UV filters, because of the hot component. In the K band, symbiotics have absolute magnitude in the range -2.5 and -7.5 (Munari & Zwitter 2002). The expected UV magnitude range in the F275W filter can be inferred from the UV magnitude at the near peak wavelength (2600 Å) indicated by Kenyon & Webbink (1984) for Galactic symbiotics: It is about 1-1.5 mag fainter than the V magnitude. The magnitudes in the Kenyon & Webbink article were not corrected for reddening, and since the average absorption of the Galactic symbiotics is higher than towards M31, we expect even a smaller difference between optical and UV magnitudes in Andromeda. The known Magellanic Clouds symbiotics are unusually bright, apparently containing mostly AGB stars, in the range V=(-2.2)–(-3.4) and with B-V$\leqslant$1.3. All symbiotics are very luminous in Hα (see Gonçalves et al. 2006, and discussion therein). We obtained Hα images of the M31 core with the WIYN telescope (see e.g. Orio et al. 2010) and also examined the archival Hα images in the LGS, but we found that the transient SSS of our group of sources are in field effected by excessive diffuse light for ground based photometry.

3 A SAMPLE OF INTRIGUING SSS

Fig. 2 shows the position of the SSS we investigated, on the scan of a plate of M31 taken with the Asiago 1.8m telescope by L. Rosino. All objects are within 5 arcmin of the inner core of M31. At the time we wrote this article, there were sufficiently deep HST archival images to observe the optical counterparts of seven SSS in M31, four of which are persistent sources (with some short lasting, recurring "off" states for r3-8). The persistent sources, likely to be steady accretors, are are most likely detectable at other wavelengths. Since all optical novae undergo an SSS phase (albeit at times effected by excessive intrinsic absorption for detection) and they are the largest class of SSS in M31 (Pietsch, Freyberg & Haberl 2005; Orio et al. 2010; Henze et al. 2014b), we must be aware that most transient SSS do belong to this class, and their optical counterpart may not be recovered in the PHAT in many cases.

The color magnitude diagrams (CMD) of the objects in Field 10 of Brick 1 of the PHAT (containing the source r2-12), obtained from the catalog of Dalcanton et al. (2012), is shown in Fig. 3. This field is quite central, crowding is particularly severe, so the upper limit magnitudes above a 4σ level in optical and IR are quite higher than in the outer regions: about magnitude 25.1 in the F475W filter, magnitude 24 in the F814W filter, and only around magnitude 20 in the F110W filter. From the theoretical isochrones also plotted in Fig. 3 we can immediately see that, despite previous conclusions that there is a mixture of populations in the M31 inner core, young stars in this extended inner core region are very rare and almost all the population has been formed between 8.6 and 9.4 Gyears ago. A complete discussion of this result can be found in Dalcanton et al. (2012). High mass binaries are thus unexpected in this region, and indeed none of the SSS we are going to describe turned out to be a member of this interesting subclass.

In the following context we use the names of the *Chandra* catalog adopted among other authors by Di Stefano et al. (2004). Source PFH 446 was observed only with *XMM-Newton*, and we refer to the catalog of the paper by Pietsch, Freyberg & Haberl (2005). The X-ray detections and some characteristics of these SSS have been reported by Di Stefano et al. (2004); Orio (2006); Orio et al. (2010).

3.1 SSS observed in the PHAT

Our SSS can be divided in three groups: persistent hot and luminous sources, persistent sources at the low end of the luminosity distribution, and transient objects that, as we already mentioned, are likely to have been optical novae.

The first of the persistent "dim" sources, **r2-54** (Di Stefano et al. 2004), was only marginally detected in an observation of 2001 and many later observations (Hofmann et al. 2013). It was still detected at at the beginning of 2011, although Hofmann et al. (2013) find that it should lower absolute luminosity than the canonical SSS (around 10^{35} erg s^{-1}) and several of the *Chandra* observations between 2006 and 2011 yielded only upper limits (see Hofmann et al. 2013). The source confusion in the *XMM-Newton* fields prevents clear detection, so we rely only on Chandra data for this source.

r2-65, initially detected in 2001 (Di Stefano et al. 2004; Orio 2006; Orio et al. 2010), is also very close to the M31 inner core. In Orio (2006) and Orio et al. (2010) it was described as a transient source. However, Hofmann et al. (2013) show that it was often observed again in *Chandra* HRC-I images between 2008 and 2012, and with the latter authors' assumptions on N(H) it would also have X-ray luminosity below 10^{36} erg s^{-1}, like r2-54 (Hofmann et al. 2013). The non-detections have upper limits above 10^{36} erg s^{-1}, so the luminosity may have decreased below this threshold when it was not detected.

The first of the transients, **r1-35**, was first noticed as a possible candidate remnant of the nineteenth century supernova S And of 1885 as discussed by Di Stefano et al. (2004); Hofmann et al. (2013). The supernova identification had already been examined and rejected by Kaaret (2002), who noted instead a transient bright counterpart in HST images of June 1995, a likely nova in outburst. Pietsch, Freyberg & Haberl (2005) suggested the association with Nova M31 1995-09b, which is in the same position of Kaaret's transient. Given that M31 can be observed only at the end of the

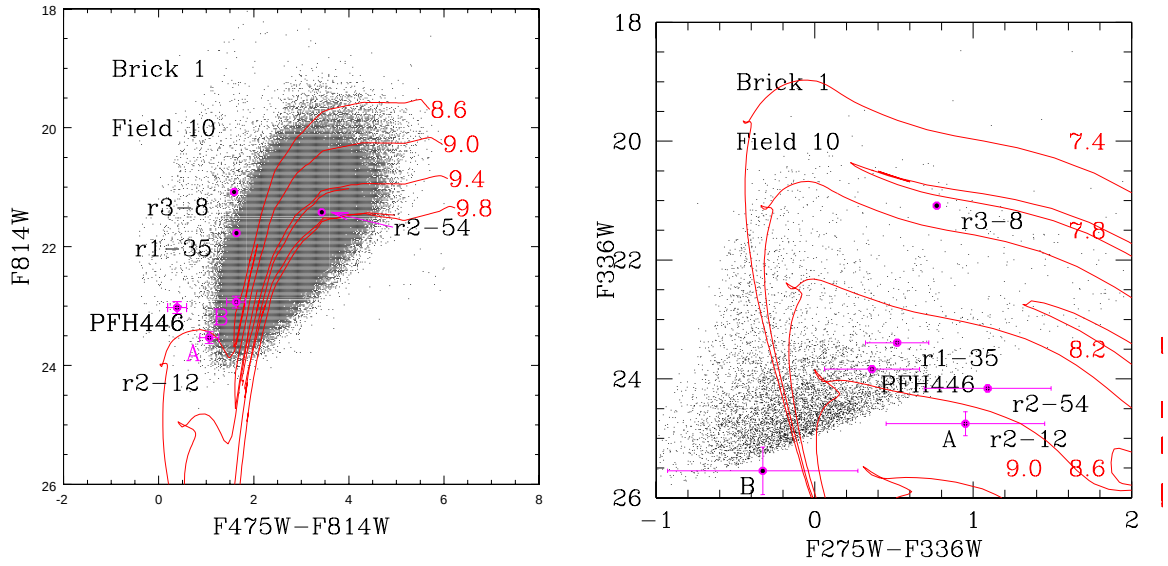

Figure 3. A set of isochrones ranging in age from 9.8 Gyr to to 7.4 Myr superimposed on the color magnitude diagrams in the optical and UV filters of the field 10 of Brick 1, containing r2-12. We also show the positions of the "candidates" discussed below. We have "reddened" the isochrones assuming E(B-V)=0.08. We have cut the optical color magnitude diagram to include only the reliable measurements, without the objects in the larger photometric catalog with less than 4 σ detections. In the UV, because the measurements are not crowding limited, we have included the measurements with large error bars.

night in the Summer and that many ground based telescopes in the Northern hemisphere are effected by poor weather in the Summer, it is very likely that the nova was discovered from the ground only in September although the outburst occurred in June or earlier. The supersoft transient was observed only almost 3 years later, but this is not unusual, especially for the M31 novae (Henze et al. 2014b). The X-ray luminosity of r1-35 was only $\simeq 3 \times 10^{35}$ erg s^{-1} (Hofmann et al. 2013), which may be consistent with a nova caught during the decline from peak X-ray luminosity, or with a soft X-rays emission lines spectrum from the ejecta (e.g. T Pyx, Tofflemire et al. 2013). It is also consistent with the overall M31 nova population statistics presented in Henze et al. (2013).

r3-115 was a peculiar transient SSS: it appeared as a typical very soft SSS in *Chandra* ACIS-S observations in 2001, but 107 days later it showed also a hard component. The X-ray spectrum became harder when it decreased in luminosity, more consistently with a black-hole transient than with a nova or other WD binary. A possible association with Nova M31 1998-07d seem unlikely because of the spectral evolution and the time lag (if a hard component is observed, it is usually in a fast nova, e.g. RS Oph).

PFH 446 was a transient only detected in *XMM-Newton* observations (Pietsch, Freyberg & Haberl 2005) and the spatial uncertainty in the position is much larger than for the *Chandra* sources, about 2 arcsec.

Finally, there are two very luminous and better studied sources, r2-12 and r3-8. **r2-12** is a very luminous, persistent SSS in the central region of M31. It has two important characteristics: a modulation with a period of 217.7 in the X-ray light curve, (Trudolyubov & Priedhorsky 2008; Orio et al. 2010), and, assuming it is a WD, a very hot atmospheric temperature, $\simeq$ 700,000-900,000 K in different exposures (Orio et al. 2010 and references therein, Henze et al. 2013). The luminosity varies from a few times 10^{37} erg s^{-1} to a few times 10^{38} erg s^{-1}. The supersoft X-ray flux modulation is likely to be the spin period of a massive WD, spun up by accretion. Another possibility is that of non-radial g-mode pulsations (see e.g. discussion by Leibowitz et al. 2006). These short period oscillations are frequent in SSS where all evidence points at "canonical" hydrogen burning WD. Multiple periods were observed in the supersoft X-ray source post-nova V4743 Sgr; they were attributed to both WD rotation and non radial oscillations (Leibowitz et al. 2006). The RN RS Oph and KT Eri in the supersoft X-ray phase displayed a modulation with a $\simeq$35 s period (Beardmore et al. 2010; Osborne et al. 2011), a period of 54 s has recently been measured in nova V339 Del (Beardmore, Osborne & Page 2013; Ness et al. 2013), and the X-ray SSS flux of CAL 83 is modulated with a 67 s period (Odendaal et al. 2014). It is very intriguing that r2-12 has been X-ray luminous for about 25 years, since the first observations of M31 with *Einstein*, and it has always been observed as one of the most luminous X-ray sources in all pointings of the M31 core with all imaging X-ray telescopes, albeit with a modest level of variability (see e.g. Hofmann et al. 2013). In the next Section we briefly analyze the variation of the X-ray period in the X-ray database of HEASARC, and discuss a limit on the period derivative.

The only other long lasting SSS with near-Eddington luminosity and effective temperature T_{eff} above 400,000 K are CAL 83 in the LMC and the symbiotic SMC 3 in the SMC. CAL 83 seems to be a massive WD with a companion with M=1.5-2 $M_\odot$ (van den Heuvel et al. 1992), an orbital period of a day (Smale et al. 1988) and T $\simeq$550,000 K (Lanz et al. 2005). The X-ray flux of CAL 83 is modulated with a 35 min period (Schmidtke & Cowley 2006) in addition to the 67 s period mentioned above. Occasionally, this source shows an "X-ray off" state for at least a week. SMC 3 has an orbital period of 4.5 years and T_{eff} $\simeq$450,000 K (Orio et al. 2008 and references therein). It also shows brief states of very low X-ray luminosity, always at the same orbital phase. Both sources, like r2-12, were initially observed with *Einstein* and were always observed as SSS throughout the last $\simeq$30 years. Despite some variability, r2-12 has always appeared above the detection threshold of the existing observations.

r3-8 is a luminous variable source: it usually has an X-ray luminosity above 10^{37} erg s^{-1}, but it also displays "off" or "low" states, falling below luminosity detection thresholds (depending on the image) of 10^{34}-10^{35} erg s^{-1} for a few weeks at a time (Orio et al. 2010). It has been detected as one of the bright M31 sources in a very large number of observations since *ROSAT* times. The association with an Hα emitting object of the LGS (Massey et al. 2006) has been suggested by Hofmann et al. (2013). This proposed counterpart is in front of a dust lane, where background sources have an extremely low probability of detection (see Orio et al. 2010).

3.2 The 217.7 s modulation in the X-ray flux of r2-12

Given the rich database of X-ray observations in the HEASARC archive, stretching through more than 25 years and including frequent exposures in the last 10 years, we measured the X-ray period in a subset of X-ray exposures with the aim of determining a period derivative and constrain the models. Trudolyubov & Priedhorsky follow a model proposed by King, Osborne & Schenker (2002) to explain a longer period SSS observed in M31, described in detail by Osborne et al. (2001). The latter, however turned out to have a very brief transient life (it was not detected again after a few months) and therefore it was almost certainly a nova (see discussion by Orio et al. 2010). Trudolyubov & Priedhorsky assume that r2-12 is accreting as an intermediate polar (IP), residing in a binary in which the donor is more massive of the WD, as in the model of van den Heuvel et al. (1992). In the King et al. scenario, accretion is occurring through a Keplerian disk, but the WD has a sufficiently strong magnetic field to be on its way to becoming a polar, where eventually accretion occurs only to the polar caps. Even in this disk-fed stage, the authors foresee that the polar caps are significantly hotter and more luminous than the rest of the WD atmosphere (even if thermonuclear burning may be occurring everywhere at the base of the envelope accreted by the WD), so the modulation of the flux is due to temperature difference at the poles. Assuming $\dot{m} = 5{\times}10^{-7}$ M$_\odot$ year^{-1}, an accretion rate that explains the supersoft X-ray luminosity as due to nuclear burning fueled by high $\dot{m}$, the maximum spin up rate to transfer all the accreting material momentum to the WD is $\mid \dot{P} \mid \lesssim 0.065$ s yr^{-1}.

The periodic signal is not detectable in all the observations we examined. Four *XMM-Newton* observations spaced by 1 day and lasting from 20 to 30 ksec were done in July of 2004, but the period is detected above a 3 σ significance level only on 2004 July 16 (see Table 3). In order to constrain the measurement of the periodic signal, and to assess if it changed in time, we examined the available pointings carried out with *XMM-Newton* and with the *Chandra* HRC-I camera, choosing those with an exposure time longer than $\sim$ 20 ks, (shorter exposures result in estimates affected by high uncertainty). We did not examine any *Chandra* ACIS-S images, where the source measurements yield a low count rate; neither the ACIS-I images in which the count rate is even much lower for this soft source. We extracted the two longest HRC-I exposures a pointing done on 10-31-2001 (47 ksec) and one of the 2011 July observations (21 ksec) with CIAO V4.6, but we did not measure any period with a significance above 3 σ in these images. Thus, at this stage, we decided to examine *XMM-Newton* exposures, in which the count rate is higher. The details are reported in Table 3.

We avoided pointings in which solar flare contamination was dominating in more than the half of the exposure time. We obtained a baseline of approximately 12 years with roughly one pointing per year, with a total of 10 observations. The *XMM-Newton* data were processed with XMM-SAS version 13.0.0, with the latest calibration file (CCF) available in November 2013. During all observations, both the pn and the MOS cameras were operating in full frame mode, but the analysis reported here is only based on the pn, which yielded a much higher S/N and has a time resolution of 73.4 ms compared to 2.6 s of the MOS. Standard data screening criteria were applied in the extraction of scientific products. We excluded from the analysis the intervals of solar flares, and used the screening criteria PATTERN=0 and FLAG=0 to obtain light curves in the 0.15-1 keV range (the source has practically no residual flux at higher energy). We extracted the source photons from a circular region of radius 20" centered at the best source position, with the exception of the few cases in which the source is extremely close to the edge of the CCD, where instead we used a circular region of radius 12.5". The background was selected from a circular region of 40" in a region in the same CCD as the source lies. The source event arrival time of each observation, in the 0.15-1 keV energy range were converted into barycentric dynamical times with the SAS tool BARYCEN.

We first computed the power spectrum and verified the presence of a peak around 4.6×10^{-3} Hz, then we estimated the periodicity of the peak by means of a phase-fitting technique (see Dall'Osso et al. 2003, for details). Due to the sparse observational coverage, the measurements, shown in Table 3, are independent and not phase connected. We note that the results for the first four observations in Table 3 are fully consistent with those of Trudolyubov & Priedhorsky (2008).

Fig. 4 shows the evolution of the period with time. We first performed a fit with a constant period, obtaining a period of 217.76 ± 0.05 s with a reduced $\chi^2_\nu = 0.57$ for 9 degrees of freedom. We concluded that the signal was constant within the uncertainty. The 3 σ upper limit on the derivative of the period, obtained by performing a fit with a constant plus a linear function, is $< 8.2 \times 10^{-10}$. This upper limit corresponds to $\mid \dot{P} \mid \lesssim 0.026$ s yr^{-1}, almost a factor of 2.5 lower than the estimate obtained assuming the the Trudolyubov & Priedhorsky model. In the model assumed by these authors, an IP with an orbital period of several hours, the upper limit on the period derivative translates into an upper limit in the mass accretion rate, $\dot{m} \leqslant 10^{-7}$ M$_\odot$ year^{-1}, which is consistent with steady hydrogen burning (e.g. Fujimoto 1982; van den Heuvel et al. 1992, and references therein).

4 THE PHOTOMETRIC RESULTS

Using the PHAT photometric catalog, in Fig. 4, 5 and 6 we plotted two sets of CMD, the optical ones (already seen for r2-12) and the UV, for Brick 1 in which most of our SSS are located. The plots also show the measurements for some candidate counterparts that we will examine further below. The CMD diagrams on the left are almost equivalent to the often used CMD plots of I vs. (B-I) and B vs. (U-B), since the used HST filters have almost the same bandpass as these Johnson filters. However, caution is needed in the comparison because translating the system of the HST filters to the Johnson system is rather complex and a precise transformation formula has not been found. For details see Sirianni et al. (2005). The angular dimensions of each optical field are 202"x202", for the WFC3+UVIS the dimension is 162"x162", and for the WFC3 IR channel it is 123"x136". In Fig. 4, 5 and 6 we indicate the sources in the spatial error circle of each SSS with the red circles. We also plotted the position of SMC 3, which has the same reddening as most of these SSS (see Table 2), for comparison. We adopted Cardelli's et al. extinction law (Cardelli, Clayton & Mathis 1988) and

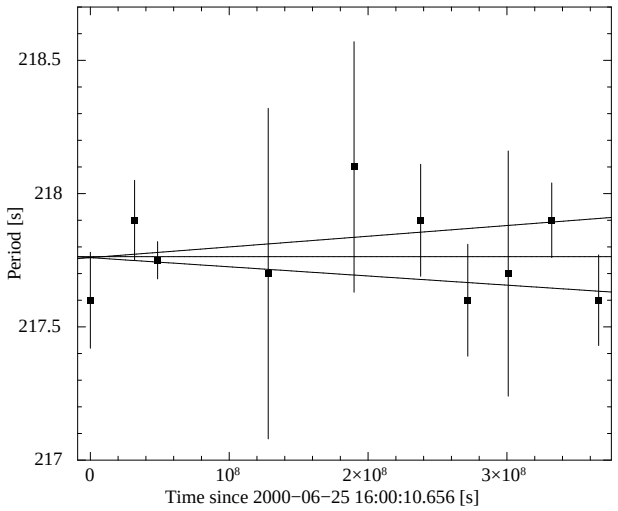

Figure 4. X-ray period of r2-12 as a function of time. The central solid line shows the fit with a constant value 217.75 ± 0.05 s, while the the top and bottom lines represent the 3σ limits on the period derivative $|\dot{P}| <= 8.2 \times 10^{-10}$. The reference time corresponds to the mid-exposure time of the first analysed dataset (observations no. 0112570401 of *XMM-Newton*).

an average value E(B-V)~ 0.08 mag in Brick 1, while we assumed E(B-V)~ 0.10 for source PFH 447 in Brick 7. These values are based on work done by Unwin (1980) and although we expect that more precise estimates will become available in the next years (see e.g., for the central 2200 pc, Dong et al. 2014), the identification of possible counterparts is not affected very significantly by the value of the reddening we adopt, which is always small. Comparisons with the best candidates for five of the SSS are shown in Table 2.

Table 4 (available on line) shows the multi-band photometric measurements for the objects detected in HST images within the spatial error circle of the SSS. We immediately note the absence of optical counterparts more luminous than 19th mag in all fields, and more luminous than 21st mag in several of them. Moreover, the vast majority of the possible counterparts are red stars, with colours typical of Asymptotic Giant Branch (AGB), red giant and supergiant stars in M31. We will discuss the exceptions below.

Generally, a foreground X-ray source emitting very soft X-ray flux would be more luminous than 21st magnitude at optical wavelengths. The first class of very soft foreground X-ray sources are AM Her systems, or polars. In a survey of ROSAT-identified magnetic CV by Pretorius, Knigge & Schwope (2013), all polars within 750 pc from the Galactic plane are at most 10 times more X-ray luminous than r2-12. Polars emitting the same X-ray flux as r2-12, but located in the Galaxy (thus with orders of magnitude lower absolute X-ray luminosity than r2-12), have an optically bright counterpart at least in the F474W filter. In the error circle of r2-12 the only optical counterparts measured with sufficient precision have colors of red giants (or subgiants, as we discuss below). We conclude that the lower limits on L_X/L_{opt} ratio for all SSS here examined, including the two dim ones, are larger than any foreground polars (see also discussion by King et al. 2002 for another M31 SSS).

The other class of very X-ray soft foreground sources are cooling neutron stars, with their thermal emission. However, they are observed only within ≃300 pc from the Galactic plane, and at such distance also they would have detectable counterparts with much "bluer" colours than the red giants. Perhaps the less optically bright neutron stars with a thermal component may be Geminga, which was discovered because of his gamma-ray emission and pulsars' properties, but according to some authors has a second component originating on the neutron star surface (Kargaltsev et al. 2005). At about 250 pc, Geminga has an optical counterpart with R≃25.5, still within the PHAT detection limits. Thus, a first conclusion is that foreground sources are very unlikely counterparts for the whole group of SSS we are examining here.

4.1 Astrometry

For most objects we report the positions of Kaaret (2002), who improved the absolute positions of sources r2-12, r3-8, r2-65, r1-35 and r3-115 in the Chandra images of the High Resolution Camera (HRC, uncertainty of 1") registering them with objects in the 2MASS catalog, so that the final coordinates differ from the 2MASS positions by at most 0.4". We estimate that this is approximately a 1σ positional uncertainty, although Kaaret further improved by applying an average coordinate shift between the HRC and 2MASS of 0.2", obtaining an average systematic displacement of only 0.15" from the 2MASS positions. Kaaret's positions differ by up to 0.23" by the positions determined by Hofmann et al. (2013) in other, more recent HRC-I images for the same sources. The 1σ uncertainty estimate in the positions of Hoffman et al. (2013) is 0.38". The position of two of the persistent sources, r2-12 and r2-54, were also measured in the Chandra ACIS camera observations of Kong et al. (2002) and we adopt the ACIS position for r2-54. These authors registered the images using the absolute positions determined by Kaaret (2002), thereby also obtaining a maximum difference from the 2MASS positions of 0.4". We note that the r2-12 position measured by Kaaret is 0.33" distant from the one obtained by Kong et al., although it is within the error circle of the former.

The release notes of the HST Legacy archive indicate an error of about 0.4" in the HST/2MASS image registration. By combining two 1 σ errors of 0.4", we evaluate that our 1 σ error circle has a radius of ≃0.6" in the relative Chandra/HST positions. For Brick 9 we found the largest difference from the 2MASS positions (a systematic shift of about 0.08" in right ascension and 0.2" in declination in the U/UV images) and we re-registered the images with MASS. For PFH 446, the SSS that was only observed with *XMM-Newton*, the source the position uncertainty is about 3". All the 1 σ relative position uncertainties estimates we gave here are very conservative.

5 THE CANDIDATE COUNTERPARTS

In Table 4, which is available in the online Journal, we list the objects detected in the spatial error circles of 6 of the SSS of our sample, in regions with photometric measurements published by the PHAT collaboration (Dalcanton et al. 2012). The "hottest" object, with the larger (U-B) and/or (UV-U) color index, has been listed first, while the other objects are in order of increasing declination.

5.1 The persistent SSS

In Table 2 we report UV/optical/IR absolute magnitudes, and color indexes for three well studied symbiotics of the Local Group that are steady SSS, and for several candidate counterparts of our SSS. We have chosen the apparently "hotter" object in the fields. However, candidate "A" in the r2-12 error circle. is *not* a good candidate

SSS, although it is the the "bluest" optical object within 0.7 arcseconds of the *Chandra* position of r2-12 detected with the UV filters. All the other objects in the spatial error circle of r2-12 have typical colors of evolved cold stars, except the "B" candidate of Table 4 and Fig. 2, which however was measured with large errors in the U filters and does not appear to be sufficiently luminous in the F275W filter to be an SSS.

As expected, young hot stars are absent. Table 2 also shows the $(B\text{-}J)_0$ color index, useful for comparison with supergiants of OB type (see Wegner et al. 1993). If r2-12 was a symbiotic system, it would have a counterpart with color indexes close to those of SMC 3 (see discussion above and Orio et al. 2007). Lin 358, Draco C-1, and AG Dra have effective temperatures around 200,000 K, which is too low for a meaningful comparison with this SSS. "Candidate A" in the Table has too large a negative value of $(U\text{-}B)_0$ compared with all the SSS-symbiotics in the Table, even the low temperature ones. For candidate "B" this color index is even much more negative.

No PHAT-detected object, including candidates "A" and "B", stand out in an Hα image of the field, taken with HST for another program. From a comparison with the off-band, the magnitude of all objects detected with this filter is in fact consistent with only continuum emission. All in all, in the spatial error circle of r2-12 we cannot identify the "signature" of a hot symbiotic that may have ongoing hydrogen burning. Candidate "A" seems to be a subgiant star at ≃8.6 Gyears. The subgiant phase is very short lived, but clearly it is not impossible to observe. Candidate "B" has been measured with great uncertainty with the F275 W filter, in which it appears faint.

If r2-12 is not a symbiotic, it is likely to be instead a short period binary ($P_{orb} \leqslant 1$ day) with characteristics similar to CAL 83, specifically high effective temperature, near-Eddington X-ray luminosity and persistence over many years. We reported that the range of absolute measured magnitudes is V=-0.92-2.02 (Greiner & Di Stefano 2002): this large optical luminosity is attributed to an accretion disk, which is irradiated by the very hot primary. The hotter and more luminous is the WD, the more luminous is the disk at optical wavelength. Models of disks for WD binaries and their luminosities are discussed in Frank, King & Raine (1992); Popham & Di Stefano (1996). The optical luminosity of the known accreting and hydrogen burning WD binaries turns out to be proportional to their orbital period (Šimon 2003; van Teeseling et al. 1997).

The X-ray luminosity of r2-12 at M31 distance, in the 0.2-10 keV range, does not fall below the value 3×10^{37} erg s^{-1} indicated by van Teeseling et al. (1997) for another LMC source, RX J0439.8-6809. This SSS in the LMC does have an unambiguous optical counterpart of magnitude V≃21.6, which would be undetectable at M31 distance. The dereddened 4 σ above background upper limit for the r2-12 region of Brick 1 is $M_B \simeq 25{,}1$ and this implies an absolute visual magnitude upper limit $M_{F475W} \geqslant +0.70$ if $(B\text{-}V)_0 \simeq -0.05$ like in CAL 83. Assuming there is correlation between absolute visual magnitude of an irradiated disk and orbital period at a given X-ray luminosity of the type $\Sigma = L_X P_{orb}^{2/3} = f(M_V)$, as derived by Van Paradijs & McClintock (1994), van Teeseling et al. (1997) analyzed the period and visual magnitude values for several SSS in the Magellanic Clouds. They obtained a semi-empirical relationship $M_V = 0.83(\pm 0.25) - 3.46(\pm 0.56)\log\Sigma$ (see their Figure 3). With this relationship, the upper limit on the PHAT magnitude upper limit translates in an orbital period shorter than 169 minutes. If we search for objects detected at less than the 4 σ level, the error in the U/UV filters is larger than 0.3 mag and it is very difficult to draw any conclusion, so we assume that what we obtained here is the lowest limit on the systems we can detect.

r2-12 may even be an AM CVn type of object (see e.g. Bildsten et al. 2013 and references therein). It is tempting to attribute the 217 s period to a nonradial oscillation of the WD (Bildsten et al. 2013), but the accretor is too hot to be in the known nonradial pulsations instability strip. On the other hand, non radial g-mode pulsations, of a "putative" but still unexplored instability strip at much higher temperature have been attributed to several post-novae (see discussion by Orio (2012)).

van Teeseling et al. (1997) also discuss the constraints on the accretion disk inclination that can be derived from the absence of an X-ray eclipse. For a source like r2-12, which is sufficiently X-ray luminous that it observed to vary, an X-ray eclipse should be measurable, however it was never observed in long continuous X-ray observations with *XMM-Newton* (Orio et al. 2010). This additional constraint indicates an inclination lower than $\leqslant 75^o$, assuming of course that the modulation with the 217.73 s period is due to the WD spin and is not the orbital period of an extremely compact binary with unusually small size, such that its optical luminosity would be too low for a detection. If the 217 s period is due to the WD rotation as we have assumed so far, we do not observe any other modulation with the orbital period with a significance above 3 σ. We thus conclude that orbital modulations are not observable, so the inclination is much lower than 75^o inferred from the eclipse absence (with some assumptions, van Teeseling et al. (1997) infer an upper limit of 10^o from a missing orbital modulation for the SSS they analyzed).

In short, once we have ruled out all the red giants, supergiants and the one likely "subgiant" (candidate "A"), as likely counterparts, a missing optical detection, coupled with the lack of orbital modulation indicating low inclination, sets strict upper limits for the optical luminosity of the r2-12 counterpart, ruling out many binary configurations. If the 217.7 s period is due the to WD spin, in Section 3 we have also shown that the model of an IP in a binary with an orbital period of several hours, proposed by Trudolyubov & Priedhorsky, implies a higher rotational period derivative than the one we measured. This may be interpreted as additional evidence that r2-12 is in a binary with an orbital period below the period gap.

The other luminous persistent source in our sample is r3-8. Orio et al. (2010) did not found any optical counterpart in a deep ground based image, but Hofmann et al. (2013) noted the detection of an Hα luminous object in the LGS. In Table 2 we indicate the values for the LGS and PHAT measurements. The PHAT position is about 0.5" from the Chandra one. However, there is a systematic shift in the astrometry of Brick 7. This candidate counterpart is also very luminous in U and UV. Its colors are not very different from those for SMC 3, fully consistent with a symbiotic star with a very hot component. Most important, the photometric measurement of the LGS and the PHAT indicate that the object has brightened in all filters, by 0.5 mag or more. It is more luminous in the PHAT, even if, as we show in Fig.8, the HST images indicate that the LGS measurements may have been contaminated by unresolved nearby objects, especially in the F814W filter. In a WIYN image of 2005 Orio et al. (2010) did not detect it below B≃23 at a 3σ confidence level. It thus seem that this object is as variable at optical wavelengths as it is in X-rays.

In the crowded fields of r2-54, a source at a lower luminosity level than the canonical SSS, (a few times 10^{35} erg s^{-1}) we found an anomalous object that is luminous in the red colors, but its "UV age" appears younger than the age inferred from the optical colors.

We included it in Table 2 for a comparison with the symbiotics and symbiotic candidates.

The colors of all objects detected in the r2-65 spatial error circle are only consistent with red giants, supergiants and AGB stars.

5.2 The transients

As we expected, given the generally old population of this central region in M31, we do not find any hot young stars in the error circles of our transients sources. Thus, we ruled out transients of the new class discovered by e.g. Li et al. (2012) and discussed by Orio (2013).

If any of the persistent sources was caught during X-ray off states, and the effective temperature decreased while the radius increased, the SSS should have become luminous UV sources (see Starrfield et al. 2012) with bolometric luminosity above 10^{36} erg s^{-1}, resulting approximately in magnitude $\leqslant$-2.5 in the F275W filter while at optical wavelengths they may have been fainter than the PHAT limits. There is no object with such high UV luminosity in any of the positional error circles of the SSS we examined.

None of the optical counterparts in the error circle of r3-115 has magnitudes and color indexes that may clearly be attributed to symbiotics, accreting WD with a luminous disk, or a luminous secondary stars, suggesting that these X-ray transients were novae. Most likely, accretion at the rate needed to sustain hydrogen burning is no longer going on.

We do find luminous red stars which are also unusually luminous in the blue/UV filters in the error circles of r1-35 and PFH 446. We detect no optical/UV counterpart for the optical Nova of 1995 which was associated with r1-35. There is an interesting object is located at 0.34" from the nova position, which however is known with higher accuracy. The object detected in the PHAT, included in Fig. 2 and Table 2, matches the color indexes of the hydrogen burning symbiotics; it is at only 0.3" from the *Chandra* position. While we think that the 1995 nova counterpart is much more likely to be the right one, we include this object in the Table, as an interesting candidate hydrogen burning symbiotic.

The putative symbiotic in the error circle of PFH 446, like the symbiotic candidate for r2-35 has absolute IR magnitude $\simeq$-2 in the F110W filter, consistent with a red giant (see Fig. 4-6 and Table 2). However, the magnitude in the the F475 W filter and in the UV ones is larger than expected, probably indicating a second component producing the optical and UV flux. The counterpart in the error circle of PFH 446 is at only 0.4" from the *XMM-Newton* position, at 2000 coordinates α=00,43,25.54, δ=+41,16,17.4. As the plots in Fig. 7 show, this object is on the blue side of the red giant branch. For the dereddened absolute magnitudes and color indexes we assumed E(B-V)=0.1 and Cardelli et al.'s dependence of extinction on wavelength (Cardelli, Clayton & Mathis 1988). A search in the LGS Hα images made us rule out strong Hα emission above the continuum level. Symbiotics do have strong Hα emission; thus, the jury is still out on the nature of this candidate counterpart.

6 DISCUSSION AND CONCLUSIONS

The SSS in M31 offer a unique possibility to classify and study a statistically significant number of these X-ray sources at known distance. The SSS in binaries with characteristics similar to nova systems, but with steady instead of transient thermonuclear burning, may belong to three classes of single degenerate binaries evolving towards type Ia SN in single degenerates: 1) The van den Heuvel et al. (1992)) type binary, a massive WD with a more massive main sequence secondary, 2) Massive young binaries with a hydrogen burning WD, 3) Symbiotics. The SSS we examined here are either in the core or are very close to the central region of M31, and not surprinsingly we have not found any optical object with the colors of high mass X-ray binaries or B stars. Our group of SSS belongs to an old population, although in general SSS as a class are clearly a mixture of young and old binaries.

Objects with colors that may indicate symbiotics, are found in the error-circles of r1-35 and PFH 446. There is a more dubious "candidate" in the error circle of r2-54. PFH 446 is in a region which is not too crowded for future spectroscopic follow-up, but the proposed counterpart is fainter than 23rd magnitude. appears The ground based facilities of the future with adaptive optics should be able to obtain optical spectra and prove the physical nature of these three objects.

Source r3-8 has a unique optical counterpart that is luminous in Hα and is optically variable. It is a likely symbiotic because of the large IR luminosity, and even more luminous in the U band than SMC3. This SSS at times falls below detection limits for several weeks: this may imply recurrent thermonuclear flashes with or without mass ejection (see e.g. Fujimoto 1982). Recently, a recurrent nova has been observed in M31 with a recurrence period of only a year (Darnley et al. 2014; Henze et al. 2014a), but thermonuclear flashes with a shorter period would occur without mass ejection. Another possibility is that the X-ray and optical variability are correlated and there is a periodic obscuration or eclipse during the orbital period, similar to the phenomenon observed in SMC 3.

Only "regular" red giants are in the error circles of r2-65 and r3-115. The low X-ray luminosity measured in the last years for r2-54 and r2-65 may rule out ongoing hydrogen burning, but it does not solve the mystery of their nature, because they are extremely luminous and soft. They may be SSS with $T_{\rm eff}$ $\leqslant$200,000 K, with WD mass is between 0.4 and 0.7 $M_{\odot}$, effected by copious intrinsic absorption (see Starrfield 2012). The optical luminosity corresponds only to an upper limit of about 8 hours in in the orbital period diagram by van Teeseling et al., which would leave most short period CBSS undetected. Perhaps these two sources are quite similar to SMC 13 (Orio et al. 1994b; Crampton et al. 1997), but are more absorbed.

The upper limits on the F435 W luminosity of the possible optical counterparts of r2-12 argue against the scenario of a foreground, thermally emitting neutron star. We will also point out here that a $\simeq$ 3 minute pulsation period is extremely unlikely for a neutron star. Such long periods have only been observed in pulsars with Be companions. While a thermally emitting cooling neutron star may also be a pulsar, Be companions are very luminous foreground counterparts at optical wavelengths (Esposito et al. 2013, and references therein) and would have not be missed.

The lack of a suitable optical/UV/Hα counterpart for r2-12 is an interesting puzzle, that can be understood in fact only if this object is in a binary orbital period below 169 minutes (2.8 hours), or else irradiation effects would make the disk sufficiently optically luminous to be detected in the PHAT. This is the most peculiar of all the SSS we examined. The detected periodic modulation is difficult to interpret without a WD, and it has high $T_{\rm eff}$ and luminosity. The missing counterpart at other wavelengths leaves us with the intriguing possibility of a very short orbital period binary, like an AM CVn binary. We cannot rule out that the X-ray luminosity is due to helium instead of hydrogen burning (Bildsten et al. 2006).

Another intriguing possibility is that the 217.7 s period is or-

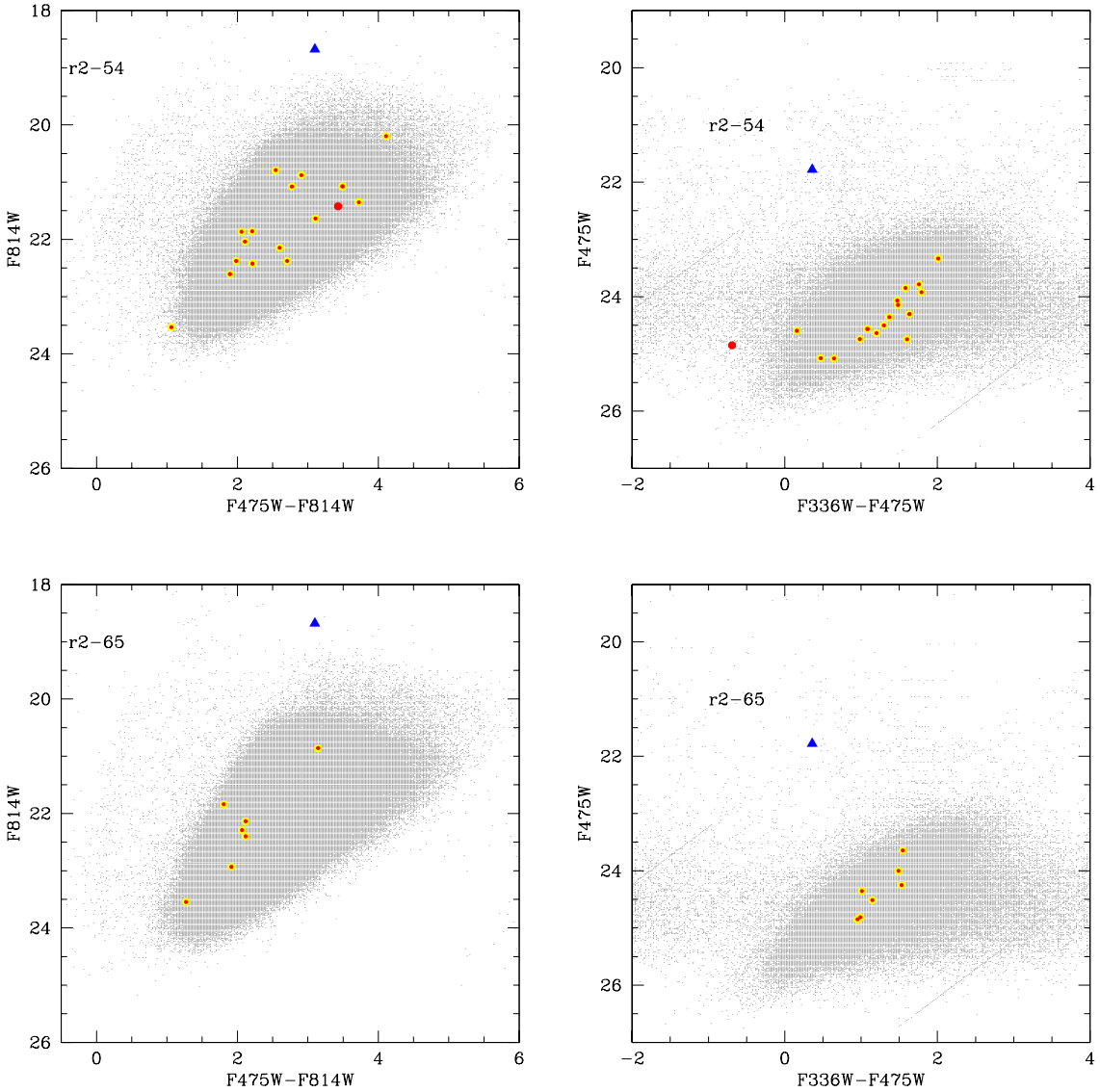

Figure 5. The position of the optical/UV counterparts in the error circle of the "dim" persistent SSS on the optical and U/UV CMD of the whole observed field, based on the Dalcanton et al. photometry. The blue triangle represents the position on the CMD of the symbiotic star SMC3 as it would appear at M31 distance. We are mainly looking for luminous red stars placed to the left than the majority of the other objects of comparable luminosity, in this plot and in Fig. 5 and 6. The most likely candidate for r2-54 is indicated with a red dot.

bital in nature. The shortest known period system is HM Cancri (which is *not* an SSS) and has a 321 s period. It is also known as RX J0806.3+1527 (Israel et al. 2002; Roelofs et al. 2010). The effective temperature of the WD in HM Cancri is about 140,000 K (Bildsten et al. 2006), much lower than the temperature inferred for the r2-12 WD. In any case, r2-12 with its high effective temperature, high luminosity and a short orbital period, is an "extreme" object and it may represent an unusual, short-lasting state at the end of binary stellar evolution. By continuing the X-ray monitoring, we will test the physics of a very interesting source, probably a key object for studies of binary evolution and SN Ia progenitors' studies.

References

Adelman-McCarthy J. K. et al., 2008, ApJs, 175, 297
Beardmore A. P. et al., 2010, The Astronomer's Telegram, 2423, 1
Beardmore A. P., Osborne J. P., Page K. L., 2013, ATel, 5573, 1
Bildsten L., Townsley D. M., Deloye C. J., Nelemans G., 2006, ApJ, 640, 466
Bonanos A. Z., Stanek K. Z., Szentgyorgyi A. H., Sasselov D. D., Bakos G. Á., 2008, Aj, 136, 896
Boyer M. L. et al., 2011, AJ, 142, 103
Burstein D., Heiles C., 1982, Aj, 87, 1165
Cardelli J. A., Clayton G. C., Mathis J. S., 1988, ApJ, 329, L33
Crampton D., Hutchings J. B., Cowley A. P., Schmidtke P. C., 1997, Apj, 489, 903
Cutri R. M. et al., 2003, VizieR Online Data Catalog, 2246, 0

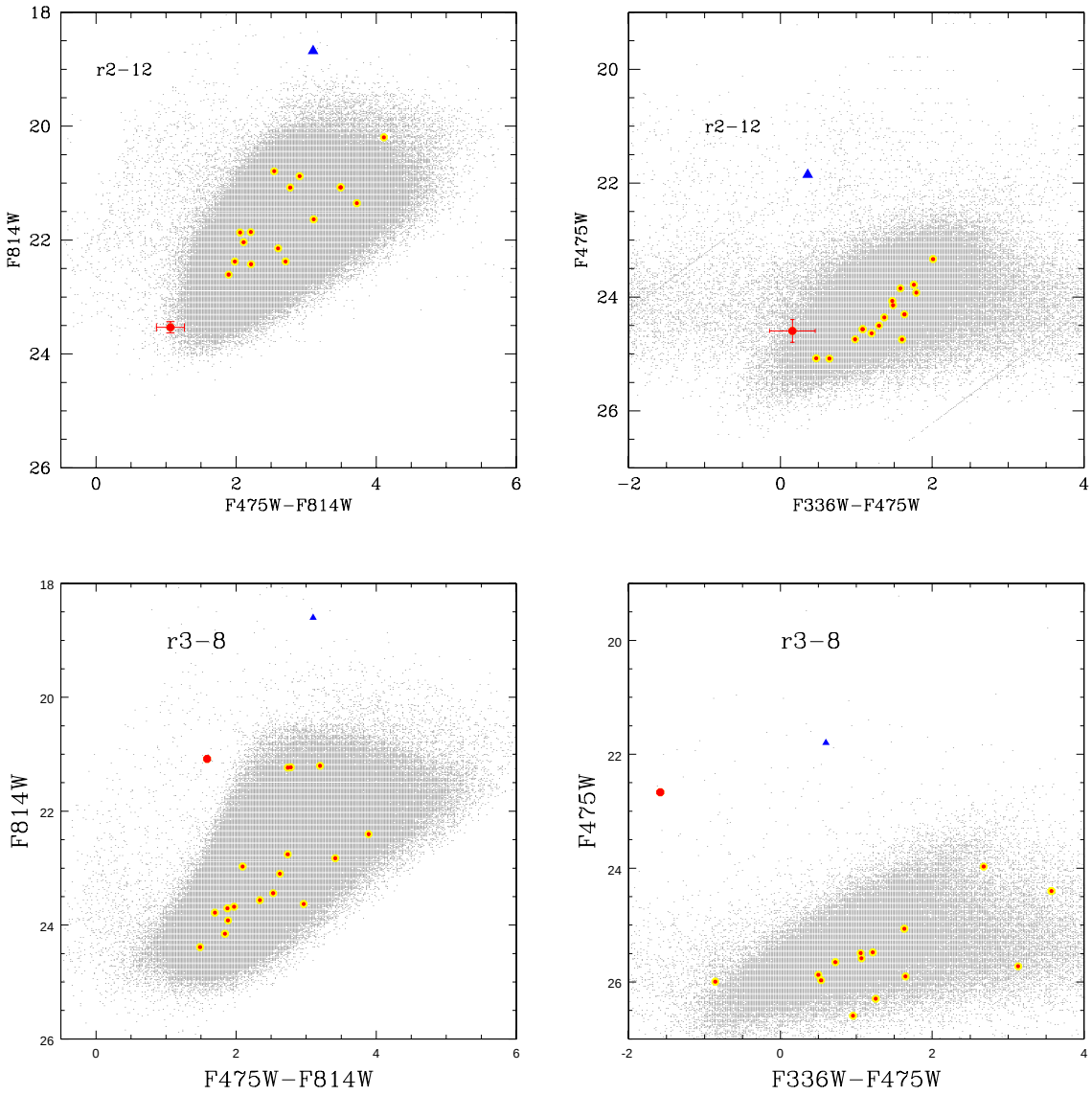

Figure 6. Position of the optical/U/UV counterparts on the CMD of the fields of the persistent "luminous" SSS, based on the Dalcanton et al. photometry. The blue triangle represents the position of the symbiotic star SMC3 as it would appear at the distance of M31. The bet candidates ("A" for r2-12) are indicated by red dots.

Dalcanton J. J. et al., 2012, ApJS, 200, 18

Dall'Osso S., Israel G. L., Stella L., Possenti A., Perozzi E., 2003, ApJ, 599, 485

Darnley M. J., Williams S. C., Bode M. F., Henze M., Ness J.-U., Shafter A. W., Hornoch K., Votruba V., 2014, ApJ, 563, L9

Di Stefano R. et al., 2004, ApJ, 610, 247

Dong H. et al., 2014, Apj, 785, 136

Esposito P., Israel G. L., Sidoli L., Mason E., Rodríguez Castillo G. A., Halpern J. P., Moretti A., Götz D., 2013, MNRAS, 433, 2028

Frank J., King A., Raine D., 1992, Science, 258, 1015

Freedman W. L., Madore B. F., Scowcroft V., Burns C., Monson A., Persson S. E., Seibert M., Rigby J., 2012, Apj, 758, 24

Fujimoto M. Y., 1982, ApJ, 257, 752

Gonçalves D. R., Ercolano B., Carnero A., Mampaso A., Corradi R. L. M., 2006, MNRAS, 365, 1039

Greiner J., 2000a, New Astr., 5, 137

Greiner J., 2000b, New Astr., 44, 149

Greiner J., Di Stefano R., 2002, A&A, 387, 944

Henze M., Ness J.-U., Darnley M. J., Bode M. F., Williams S. C., Shafter A. W., Kato M., Hachisu I., 2014a, A&A, 563, L8

Henze M. et al., 2014b, A&A, 563, A2

Hofmann F., Pietsch W., Henze M., Haberl F., Sturm R., Della Valle M., Hartmann D. H., Hatzidimitriou D., 2013, A&A, 555, A65

Inno L. et al., 2013, Apj, 764, 84

Israel G. L. et al., 2002, A&A, 386, L13

Kaaret P., 2002, ApJ, 578, 114

Kargaltsev O. Y., Pavlov G. G., Zavlin V. E., Romani R. W., 2005, Apj, 625, 307

Kenyon S. J., Webbink R. F., 1984, ApJ, 279, 252

Kinemuchi K., Harris H. C., Smith H. A., Silbermann N. A.,

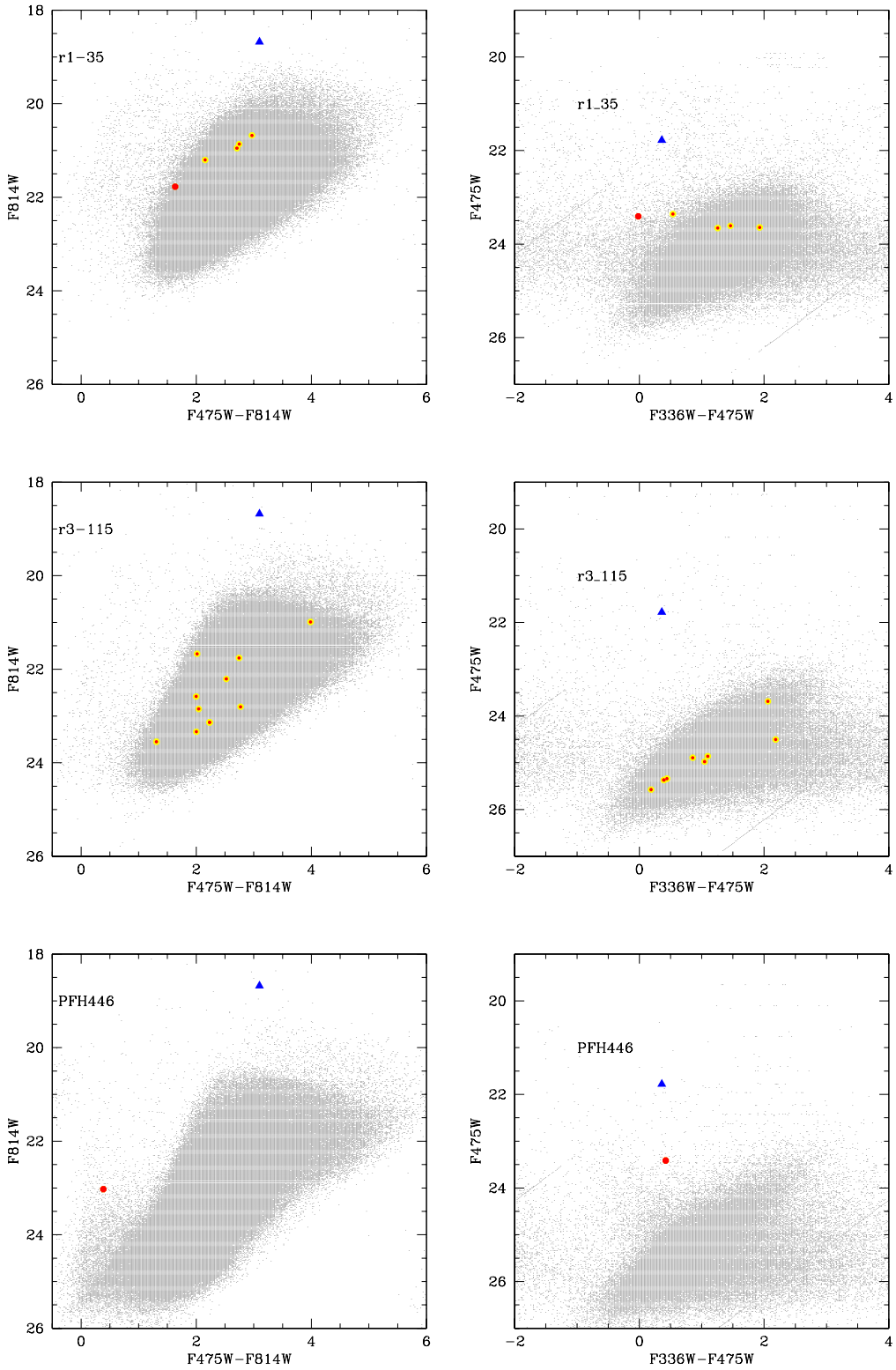

Figure 7. Positions of the optical/U/UV candidates on the CMD of the fields of the transient SSS, based on the Dalcanton et al. photometry. The blue triangle represents the position of the symbiotic star SMC3 as it would appear at the distance of M31, the red dots indicate the candidate counterparts.

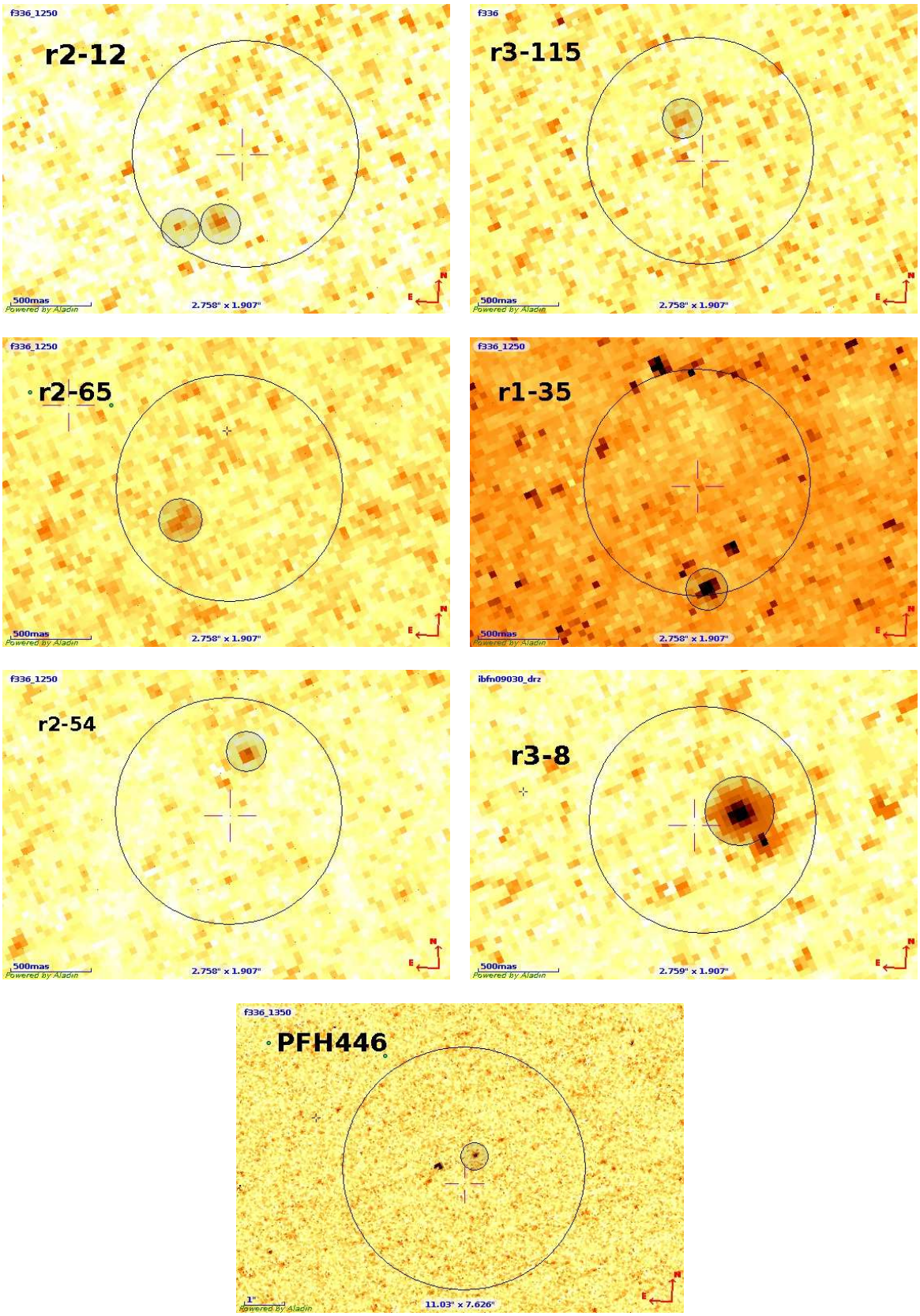

Figure 8. The fields in the F336W filter images and the spatial error circle of the X-ray positions of the SSS, with a 0.7" radius for all the source except PFH 446, for which it is of 3". We re-registered the HST image of r3-8 with 2-MASS because there is an additional systematic shift in the world coordinate system of the U/UV images of Brick 7 of the PHAT. The small circles show the positions of the selected counterparts.

Snyder L. A., La Cluyzé A. P., Clark C. L., 2008, ApJ, 136, 1921
King A. R., Osborne J. P., Schenker K., 2002, MNRAS, 329, L43
Kong A. K. H., Garcia M. R., Primini F. A., Murray S. S., Di Stefano R., McClintock J. E., 2002, ApJ, 577, 738
Lanz T., Telis G. A., Audard M., Paerels F., Rasmussen A. P., Hubeny I., 2005, ApJ, 619, 517
Leibowitz E., Orio M., Gonzalez-Riestra R., Lipkin Y., Ness J.-U., Starrfield S., Still M., Tepedelenlioglu E., 2006, MNRAS, 371, 424
Li K. L. et al., 2012, ApJ, 761, 99
Long K. S., Helfand D. J., Grabelsky D. A., 1981, ApJ, 248, 925
Massey P., Olsen K. A. G., Hodge P. W., Strong S. B., Jacoby G. H., Schlingman W., Smith R. C., 2006, AJ, 131, 2478
Munari U., Zwitter T., 2002, A&A, 383, 188
Ness J. U., Schwarz G. J., Page K. L., Osborne J. P. e. a., 2013, ATel, 5626, 1
Ness J.-U., Starrfield S., Jordan C., Krautter J., Schmitt J. H. M. M., 2005, MNRAS, 364, 1015
Odendaal A., Meintjes P. J., Charles P. A., Rajoelimanana A. F., 2014, MNRAS, 437, 2948
Orio M., 2006, ApJ, 643, 844
Orio M., 2012, Bulletin of the Astronomical Society of India, 40, 333
Orio M., 2013, The Astronomical Review, 8, 010000
Orio M., della Valle M., Massone G., Ogelman H., 1994a, A&A, 289, L11
Orio M., della Valle M., Massone G., Ogelman H., 1994b, A&A, 289, L11
Orio M., Nelson T., Bianchini A., Di Mille F., Harbeck D., 2010, ApJ, 717, 739
Osborne J. P. et al., 2001, A&A, 378, 800
Osborne J. P. et al., 2011, ApJ, 727, 124
Pietsch W., Fliri J., Freyberg M. J., Greiner J., Haberl F., Riffeser A., Sala G., 2006, A&A, 454, 773
Pietsch W., Freyberg M., Haberl F., 2005, A&A, 434, 483
Popham R., Di Stefano R., 1996, in Lecture Notes in Physics, Berlin Springer Verlag, Vol. 472, Supersoft X-Ray Sources, Greiner J., ed., p. 65
Pretorius M. L., Knigge C., Schwope A. D., 2013, MNRAS, 432, 570
Rajoelimanana A. F., Charles P. A., Meintjes P. J., Odendaal A., Udalski A., 2013, MNRAS, 432, 2886
Roelofs G. H. A., Rau A., Marsh T. R., Steeghs D., Groot P. J., Nelemans G., 2010, ApJL, 711, L138
Schmidtke P. C., Cowley A. P., 2006, AJ, 131, 600
Sirianni M. et al., 2005, PASP, 117, 1049
Smale A. P. et al., 1988, MNRAS, 233, 51
Starrfield S., Timmes F. X., Iliadis C., Hix W. R., Arnett W. D., Meakin C., Sparks W. M., 2012, Baltic Astronomy, 21, 76
Tofflemire B. M., Orio M., Page K. L., Osborne J. P., Ciroi S., Cracco V., Di Mille F., Maxwell M., 2013, Apj, 779, 22
Trudolyubov S. P., Priedhorsky W. C., 2008, ApJ, 676, 1218
Unwin S. C., 1980, MNRAS, 192, 243
Šimon V., 2003, A&A, 406, 613
van den Heuvel E. P. J., Bhattacharya D., Nomoto K., Rappaport S. A., 1992, A&A, 262, 97
van Teeseling A., Reinsch K., Hessman F. V., Beuermann K., 1997, A&A, 323, L41
Zemko P., Orio M., 2013, ArXiv e-prints

Table 1. X-ray positions of the SSS, optical/UV HST images used to search for counterparts, and dates of X-ray detection or observation with no detection (either due to variability or to complete turn-off in X-rays. The H-number added for three sources is from the article by Hofmann et al. (2013). Uncertainties in the positions are discussed in Section 4.1

Object	Position		Field	Optical Datasets		UV Datasets		Detected	Not Detected
NAME	$\alpha(J2000)$	$\delta(J2000)$	(Brick 1)	Filter	Exp(s)	Filter	Exp(s)		
r2-54	00:42:38.77	41:15:26.44	11	F814W	1700	F336W	1250	2002 Oct	often
H-106				F475W	1890	F275W	925	2005 Dec	undetected
								2006 Feb	in shallower
								2010-2012	images
r1-35	00:42:43.11	41:16:04.2	11	F814W	1700	F336W	1250	2001 Oct	2004-2012
H-146				F475W	1890	F275W	925		
r2-65	00:42:47.17	41:14:13.2	16	F814W	1700	F336W	1250	2001 Oct	often
H-194				F475W	1890	F275W	925	2008-2012	undetected
r2-12	00:42:52.50	41:15:40.1	10	F814W	1700	F336W	1250	1979-2012	
H-229				F475W	1890	F275W	925		
				F658N	2700				
r3-115	00:43:06.98	41:18:10.5	03	F814W	1505	F336W	1350	2001-2002	2004-2012
H-273				F475W	1710	F275W	1010		
r3-8	00:43:18.92	41:20:16.7	(B.7)	F475W	1720	F336W	1300	1990-2012	"off" states
H-294			(B.7)	F814W	1520	F275W	1050		(few weeks)
PFH 446	00:43:25.56	41:16:17.1	01	F814W	1505	F336W	1350	2002	2004-2012
				F475W	1710	F275W	1010		

Table 2. Absolute, dereddened magnitudes and dereddened color indexes for three known symbiotic SSS in the Local Group, for the "bluest" object corresponding to the r2-12 *Chandra* position, and of of the suggested candidate optical counterparts of r3-8, PFH 446, r1-35, and r2-54. The Johnson magnitudes are grouped together with the HST filter covering the (mostly) overlapping wavelength range. From the 4th to the 8th column, the dereneddene color indexes are in the overlapping HST filters' bands, not in the Johnson bands. The last row reports the assumed value for E(B-V). For dereddening we assumed Cardelli et al.'s extinction (Cardelli, Clayton & Mathis 1988). We did not add the smaller errors due to uncertainties in the distance modulus and the reddening. The measurements of the already known Local Group SSS-symbiotics have very small errors, that are not reported here. We adopted a distance modulus 18.93±0.02 for the SMC (Inno et al. 2013), and 19.40±0.02 for Draco (Bonanos et al. 2008).

Filter	SMC3	Lin 358	Draco C1	cand. r2-12	cand. r3-8	cand. PFH 446	cand. r1-35	cand. r2-54
FW275				+0.8±0.3	-3.085±0.001	-0.9±0.1	-1.03±0.08	0.3±0.3
F336W				-0.10±0.25	-3.765±0.001	-1.12±0.03	-1.46±0.0.03	-0.69±0.06
U	-2.60 (1)		-0.44(3)		-3.155			
F475W				-0.16±0.02	-2.08±0.01	-1.41±0.01	-1.34±0.01	-0.10±0.03
B	-3.21 (1)	-2.74(2)	-1.09(4)		-1.637			
V	-4.46 (1)	-3.40(2)	-2.34(3)					
R			-3.00(5)		-3.00			
Hα		-4.89(2)	-3.18		-2.710			
F814W				-1.06 ±0.02	-3.509±0.001	-1.60±0.02	-2.82±0.01	-3.168±0.005
I	-5.96(1)		-3.79(3)		-3.599			
F110W					-5.700±0.001	-2.63±0.02		-5.858±0.001
J	-7.10(2)	-6.53(2)	-5.05(4)					
$(B-J)_o$	+3.89	+3.79	+3.83	+7.15	+3.618	+0.91	+4.29	
$(B-V)_o$	+1.25	+0.66	+1.27		-0.062			
$(U-B)_o$	+0.41		+0.62	+0.06±0.27	-1.68±0.01	+0.28±0.04	-0.18±0.04	-0.59±0.09
E(B-V)	0.08	0.08	0.03	0.08	0.08	0.10	0.08	0.08
[1]Boyer et al. (2011),[2] 2MASS catalog, [3]Kinemuchi et al. (2008), [4]Adelman-McCarthy et al. (2008),[5]Cutri et al. (2003)								

Table 3. *XMM − Newton* observations' dates and duration and the measured periods. The uncertainty is at the 1σ confidence level.

ObsID	Start Date yyyy-mm-dd hh:mm:ss	End Date yyyy-mm-dd hh:mm:ss	Duration s	Period s
0112570401	2000-06-25 08:12:41	2000-06-25 20:59:33	46012	217.70 ± 0.18
0112570101	2002-01-06 18:00:56	2002-01-07 11:52:53	64317	217.75 ± 0.07
0202230201	2004-07-16 16:17:05	2004-07-16 21:54:04	20219	217.70 ± 0.62
0405320501	2006-07-02 14:13:51	2006-07-02 20:19:04	21913	218.10 ± 0.47
0505720301	2008-01-08 06:37:19	2008-01-08 14:10:58	27219	217.90 ± 0.20
0551690601	2009-02-04 12:56:54	2009-02-04 20:25:31	26917	217.60 ± 0.21
0600660301	2010-01-07 07:22:24	2010-01-07 12:11:00	17316	217.70 ± 0.46
0650560301	2011-01-04 17:46:08	2011-01-05 03:03:03	33415	217.90 ± 0.14
0674210601	2012-01-31 01:55:26	2012-01-31 09:08:03	25957	217.60 ± 0.17

Table 4. In this table, available in electronic format, we give the PHAT catalog coordinates and magnitudes in the different filters of the objects in the error circles of 6 of the SSS. Column 1 and 2 are the position of the objects, column 3 is the offset from the position of the sources listed in Table 1, columns 4 and 5 are the magnitudes in the optical filters, column 6 and 7 are the magnitudes in the UV filters, and column 8 is the infrared magnitude. The first raw shows the values for the "blues" candidate in each error circle, while the rest of the entries are in order of growing δ.

objects in the r2-54 error circle							
RA(J2000)	DEC(J2000)	offset(")	F475W MAG	F814W MAG	F275W MAG	F336W MAG	F110W MAG
00 42 38.77,	+41 15 26.88	0.37	24.851	21.422	25.251	24.160	18.682
00 42 38.58,	+41 15 26.2	0.3	24.498	21.27	27.551	25.421	17.845
...	...	...	...	...	...	...	...